Fire Safety Journal 138 (2023) 103794

Contents lists available at ScienceDirect

Fire Safety Journal

journal homepage: www.elsevier.com/locate/firesaf

Numerical simulations on refractory linings for steel casting vessels

Rafael G. Oliveira [a], Joao Paulo C. Rodrigues [b,c,d], Joao M. Pereira [e,*]

[a] University of Coimbra, ISISE, Department of Civil Engineering, Coimbra, Portugal
[b] University of Coimbra, CERIS, Department of Civil Engineering, Coimbra, Portugal
[c] Itecons, Coimbra, Portugal
[d] Federal University of Minas Gerais, Department of Structural Engineering, Belo Horizonte, Brazil
[e] University of Minho, ISISE, Department of Civil Engineering, Guimarães, Portugal

ARTICLE INFO

Keywords:
Refractory linings
Creep
Thermomechanical simulation
High temperatures

ABSTRACT

This paper presents an extensive numerical investigation for developing finite element models capable of simulating the thermal and mechanical response of dry-stacked masonry linings for steel casting vessels. The developed numerical models were previously validated with experimental results. The models were developed using the finite element software Abaqus. A meso-modelling approach was adopted, therefore, the units were modelled separately and connected to each other by surface-to-surface contact interactions. This work shows that the joints play an important role in dry-stacked refractory masonries reducing the stiffness of the linings and consequently reducing the compressive stresses developed in the working lining, and the tensile stresses in the steel shell. The influence of creep in the stress's development and the influence of the Young's modulus are also presented and discussed.

1. Introduction

The manufacturing of several materials adopted in industry, civil construction and our daily life has processes performed at high temperatures, such as melting and heat treatments. Thus, these production processes require products that resist to high temperatures, maintaining their physical and chemical properties in service. Refractory ceramics, due to their properties, have been used for this purpose, having crucial importance in high temperature processes. Refractory linings (composed of refractory ceramics) are used in industrial vessels to produce steel, iron, cement, non-ferrous metals, glass, metallic alloys, in melting process, in petrochemical industry, in incinerators, in mineral processing, in power plants and many other applications. The service temperature of these vessels is around 1650 °C for the steel ladles and 1450 °C for the cement kilns, however, some processes may reach 2000 °C [1,2].

Refractory linings used in industrial furnaces and vessels perform different functions [1]: a) barrier function: the refractory layers must guarantee personnel safety and protect the steel shell and the adjacent industrial facilities when operating at high temperatures; b) container function: the lining shall confine solid, liquid or gaseous substances in the containers without altering their chemical composition; c) thermal insulation function: the refractory linings shall contain the heat within the vessels and limit heat losses, contributing to the thermal efficiency of the industrial processes.

A steel ladle can have mortarless masonry (dry-stacked masonry) in its linings [3]. The relative arrangement of the bricks creates gaps between the bricks, creating a dry joint. The behaviour of such joint depends on several factors, including the surface roughness and geometric imperfections of the bricks [4–6]. Material discontinuity induced by the dry joints and its cyclic opening and closing behaviour alters the macroscopic behaviour of the masonry [7–9]. The overall behaviour of such structure is orthotropic and nonlinear, being different from the observed behaviour of its constituent materials [10,11]. Due to all these factors, comprehensive research is required to optimise the design of such linings. Of course, large-scale experimental campaigns are limited in the literature due to the cost associated with such endeavours, technical complexities and extreme working conditions involved [11–13]. This means that numerical research must be used and deployed to study the behaviour of such installations, which can then be validated with available experimental results and later used to better understand its behaviour and lead to optimal designs.

Xia and Ahokainen [14] developed a numerical model to analyse the transient heat transfer of a steel ladle during the holding period. The refractory layers (working, safety and insulation) and the steel shell

* Corresponding author.
E-mail address: jpereira@civil.uminho.pt (J.M. Pereira).

https://doi.org/10.1016/j.firesaf.2023.103794
Received 20 December 2022; Received in revised form 13 March 2023; Accepted 10 April 2023
Available online 13 April 2023

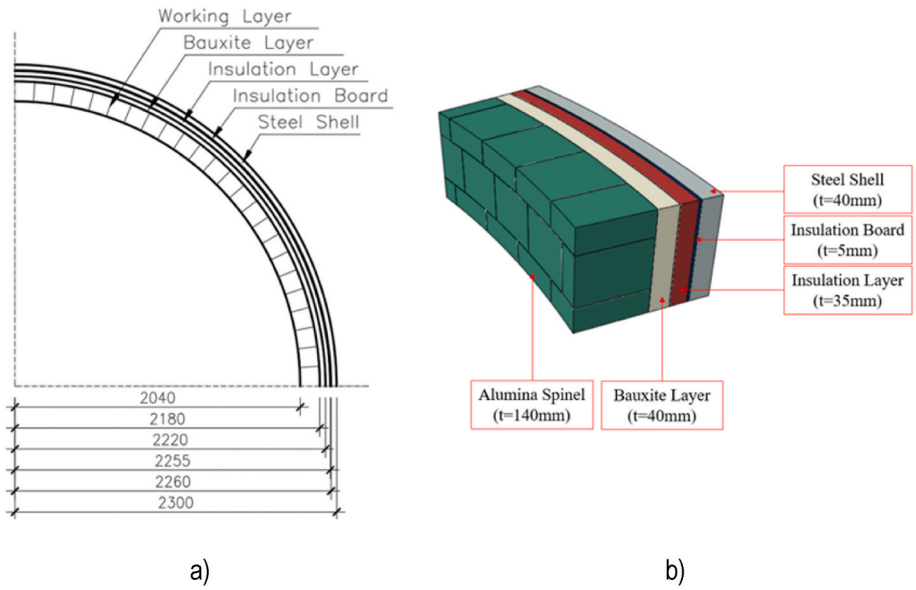

Fig. 1. Details of the steel ladle: a) dimensions of the ladle, b) details of the model.

were bi-dimensionally modelled. The heat losses in the steel shell, in the molten steel and in the exposed faces of the refractory layers were considered. The numerical predictions were validated against experimental results measured in a pilot ladle. The study was focused only on the heat transfer analysis and the mechanical behaviour of the steel ladle was not considered.

Glaser et al. [15] carried out a study like the one performed by Ref. [14] to analyse the fluid flow and heat transfer in a steel ladle. The authors also have used a two-dimensional model to predict the temperature fields in the molten steel and in the components of the steel ladle. The model was validated against industrial measurements using infrared cameras. The authors highlighted that the insulation layer plays a major role limiting the heat losses. Only the thermal fields were being analysed in this study. The mechanical behaviour of the steel ladle components was not analysed.

Although innovative results were presented by previous studies [14,15], the mechanical simulation of the vessel was not performed. In service, the refractory linings are prone different phenomena such as creep, corrosion, abrasion and fracture. The restrained thermal elongation results in elevated compression stresses in the linings and tensile stresses in the steel shell. The accurate prediction of the strain and stresses are crucial for the correct design of the structure.

Yilmaz [16] extended the previous studies [14,15] incorporating the analysis of the mechanical fields on the numerical models. The author has used a two-dimensional axisymmetric model. The simulation was carried-out using a sequentially coupled heat transfer-structural analysis. The geometry of the steel ladle was composed by a wear lining with different thickness at the barrel and at slag line, one safety lining, one insulating lining and one steel shell. The mechanical boundary condition considered the ladle lifted by a crane, as usual in the steelmaking process. Temperature-dependent mechanical and thermal properties were considered for the materials. The displacement fields were calculated; the author has identified the biggest displacement in the bottom of the steel ladle, caused by the weight of the molten steel and the refractory lining. The model presented by the author was innovative, nevertheless, it did not consider the transient heat flow of the process, as a steady-state analysis was performed to identify the temperature fields. Additionally, the author did not consider the viscoplastic strains in the refractory linings caused by relaxation.

Gasser et al. [17] used homogenization techniques to evaluate the influence of different masonry designs of the bottom of the linings. The homogenizing techniques reduced significantly the computational effort required to run the simulations, thus, it was possible to use more detailed three-dimensional models in the numerical simulations. Different masonry designs could be used in the bottom of the steel ladle, the most used are the parallel, fish bone and radial. The authors aimed to benchmark the performance of these designs in terms of stress level and displacement in the steel shell. Therefore, homogenized models of steel ladles with different bottom designs were developed. The thermo-mechanical properties of the materials were taken as temperature dependent. The authors have also evaluated the influence of the presence of the joints and the influence of the joint thickness. It was observed that the presence of joints reduced significantly the stresses generated in the steel shell, moreover, it was noticed that the radial design led to the smallest stress amplitudes in the steel shell.

Ali et al. [9] have used homogenization to simulate the thermo-mechanical behaviour of steel vessels. The developed constitutive model was validated against experimental results, and good agreement was observed. The model was used to simulate the transient thermo-mechanical behaviour of a steel ladle. Three operational cycles were simulated. The authors have performed a parametric study to analyse the impact of the joint presences and joint thickness in the overall behaviour of the ladle. An isotropic model (without joints) and models with different joint thickness (0.1 mm, 0.3 mm and 0.5 mm) were studied. The numerical predictions shown an orthotropic and nonlinear thermomechanical behaviour. The stresses originated from the restrained thermal elongation of the refractory lining decreased with the increasing in the joint thickness.

This paper presents the results of an extensive numerical investigation using finite element models capable of simulating the thermal and mechanical response of dry-stacked masonry linings for steel casting vessels. The developed numerical models were based in the results of experimental tests carried out by the authors [6,11,13].

Table 1
Materials' properties.

Properties	Alumina Spinel	Bauxite	Fire Clay	Insulation Board	Steel
Density [kg/m^3]	3130	2680	857	998	7850
Thermal elongation coefficient [/°C]	7.4×10^{-6}	7.8×10^{-6}	6.4×10^{-6}	9.3×10^{-6}	1.33×10^{-5}

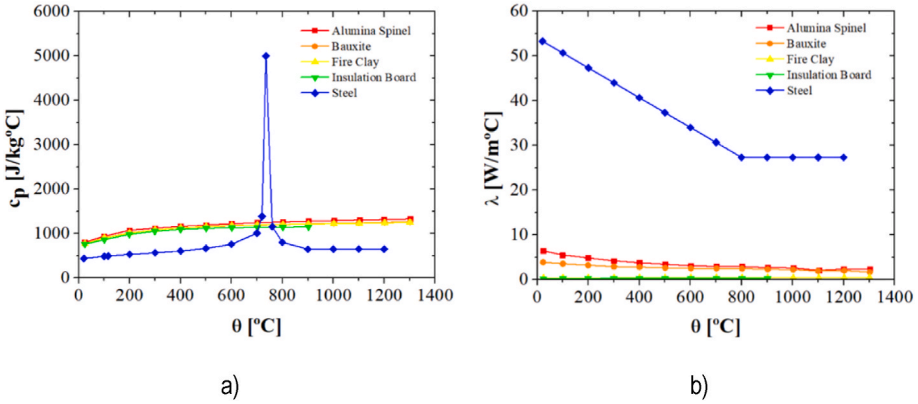

Fig. 2. Thermal properties of the materials: a) specific heat; b) thermal conductivity [18,19,27].

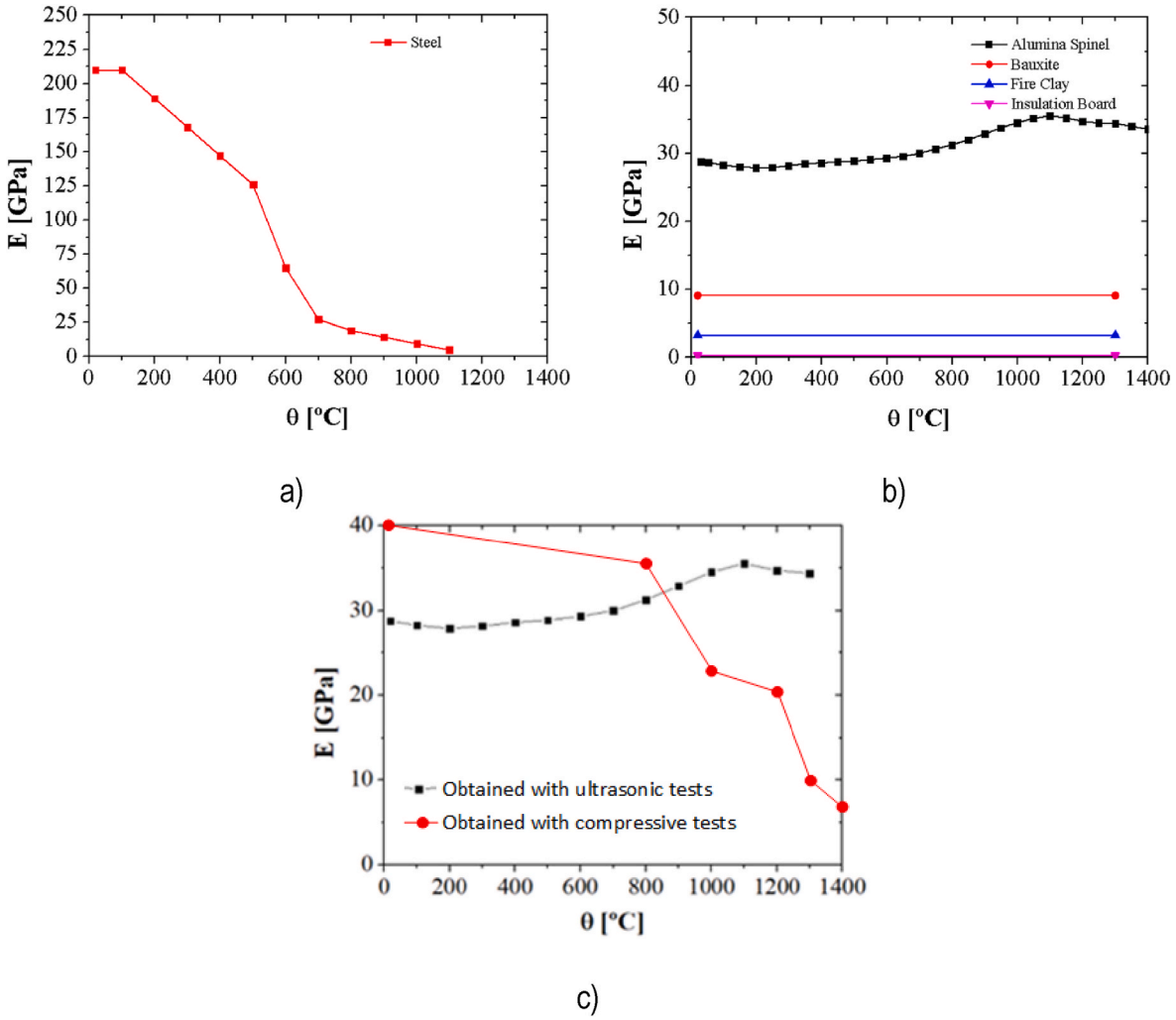

Fig. 3. Materials' Young's moduli: a) steel shell [9,10]; b) different components of the ladle [9,10]; c) comparison of Young's modulus of alumina spinel [20,28].

2. Steel ladle and components

A typical geometry of a steel ladle is shown in Fig. 1. As it can be seen, the barrel of a steel ladle is composed of different layers. Aiming already at the target ladle of this study, this typical ladle is composed by a 140 mm thick working lining (alumina spinel), a 40 mm safety lining (bauxite layer), a 35 mm thick insulation lining (fire clay), a 5 mm insulation board (medium density) and a 40 mm thick steel shell.

The density and thermal elongation coefficient of the used materials were taken as non-temperature dependent and are presented in Table 1. The specific heat and thermal conductivity are given in Fig. 2 [18,19]. The Young's moduli are detailed in Fig. 3 [9,10]. It should be mentioned that the procedure used to obtain the Young's modulus yields different results. Fig. 3b presents a comparison of the Young's modulus obtained with two different techniques. First with ultrasonic measurements [20], second with compressive tests [28]. As this is one of the variables used in

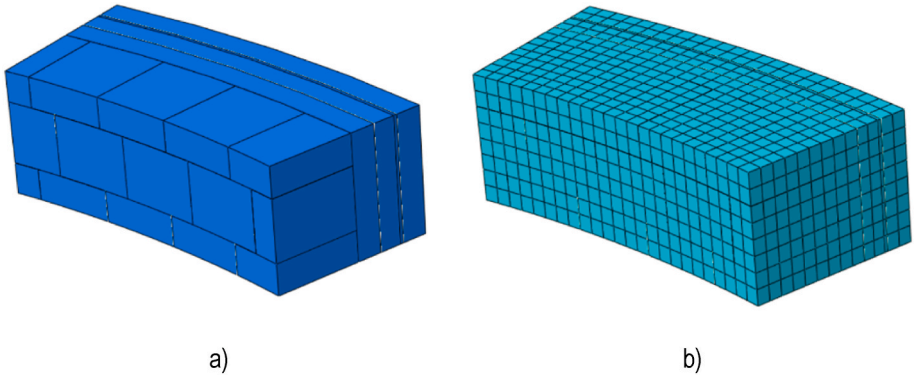

Fig. 4. Details of the model: a) general arrangement, b) mesh.

Table 2
Compressive creep parameters [23].

Temperature (°C)	n	a	Log (K/MPa-n)
1300	4.25	−2.73	−14.41
1400	5.80	−2.65	−13.90
1500	2.00	−1.97	−9.79

the numerical simulations, this will be discussed further in the following sections.

3. Numerical model

A meso-modelling approach was chosen to represent the barrel of the steel ladle. It should be noted that considering the representative section selected for this study, the bottom of the steel ladle is not considered. The bricks of the working lining were modelled separately, and surface-to-surface contact interactions were used to represent their joints. The masonry layers of the safety lining (bauxite) and insulation lining (fireclay) were built with thin-layer mortar, and they were assumed and modelled as a homogeneous material and their Young's moduli were calculated according to Ref. [21]. Aiming to reduce the computational time, the ladle was modelled as 15° slice with axisymmetric boundary conditions, with the vertical displacement being restrained. The general arrangement of the model is presented in Fig. 4a. A sequentially coupled analysis was performed. The analyses were performed with Abaqus [22] and the DC3D8 elements were used for the heat transfer and the C3D8R elements for the mechanical analysis. A mesh study was performed and led to the element dimensions of approximately 20 mm. The adopted mesh is given in Fig. 4b.

Creep (viscoplastic behaviour) plays a relevant role in the thermo-mechanical behaviour of the steel ladle. The strain hardening form of the Norton-Bailey creep law is being used to represent the creep strains in the material. The experimental results provided by Ref. [23] evidences the three-stage creep curves of the alumina spinel material. However, the present study is mainly focused on the primary creep stage. The creep strain rate may be obtained by:

$$\dot{\varepsilon}_{cr} = K(T)\,\sigma^{n}\,\varepsilon_{cr}^{a} \qquad \text{Eq. 1}$$

where σ denotes the compressive stress, $\dot{\varepsilon}_{cr}$ is the creep strain rate, ε_{cr} is the creep strain, $K(T)$ is a temperature dependent value, n is the stress exponent and a is the strain exponent. The parameters $K(T)$, a and n were inversely identified by Ref. [23] and are being presented in Table 2. It should be noted that due to the available data, creep was not considered below 1300 °C.

3.1. Joint behaviour

The joints play an important role on the behaviour of dry-stacked masonry and they were modelled with surface-to-surface contact properties. The joints' normal behaviour was represented by a pressure-overclosure relation. In this formulation the contact stiffness increases with the overclosure of the joint, resulting in a suitable representation of the behaviour of the dry joints. The behaviour of the dry-stacked masonry varies with the size of the specimen [24], consequently, different relations might be used to represent masonry with different dimensions (Fig. 5a). The general formulation provided by Ref. [25], was used to model the joint behaviour. Based on the work developed by Ref. [11], the pressure-overclosure relation used within these numerical simulations can be seen in Fig. 5b.

The tangential behaviour was represented by the penalty friction formulation, in which sliding is governed by the friction coefficient. The

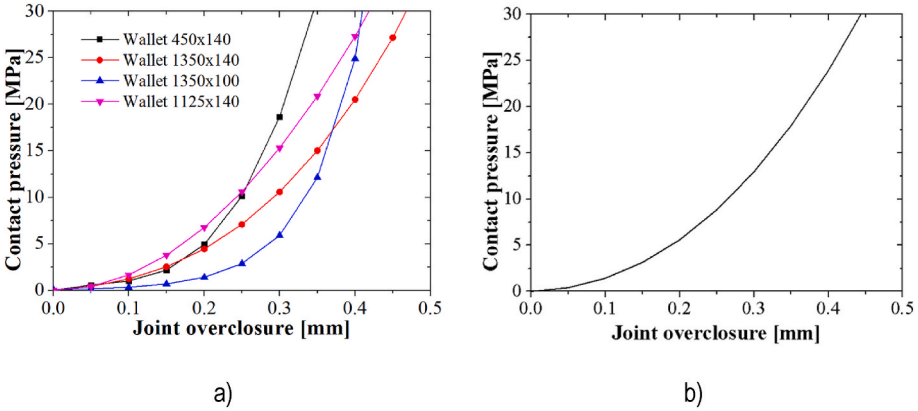

Fig. 5. Contact pressure-overclosure relations: a) obtained experimentally by Ref. [11] for different wall dimensions; b) relation used in this study.

Table 3
Friction coefficient values for dry joints and different temperatures [6].

Temperature [°C]	Friction Coefficient [−]
20	0.598
300	0.498
600	0.510
900	0.530

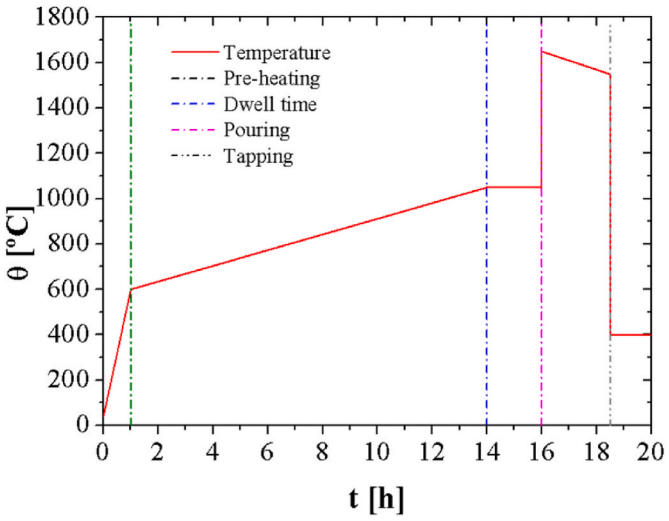

Fig. 6. Thermal cycle of the steel ladle.

friction coefficient of the alumina bricks as a function of the temperature was obtained experimentally by Ref. [6] and it can be seen in Table 3.

3.2. Thermal load

The steel ladle was submitted to a thermal cycle composed by: i) pre-heating from 40 °C to 600 °C in 1 h; ii) pre-heating from 600 °C to 1050 °C in 13 h; iii) dwell time of 2 h at 1050 °C; iv) steel pouring and treatment for 2.5 h, in this period the temperature of the molten steel decreases from 1650 °C to 1550 °C; v) waiting time at 400 °C for 2 h. The thermal cycle is detailed in Fig. 6. The emissivity of the alumina spinel and the steel shell were taken as 0.70 [26,27]. The convection coefficient was taken as 8 W/m^2°C, as usually defined for natural convection [27]. The emissivity and convection coefficient were assumed to be constant with temperature.

3.3. Validation

In order to gain confidence in numerical results, models should be validated with experimental results. The modelling approach described in this paper has been validated with experimental tests under different conditions. This model was used to replicate some experimental tests performed within the framework of the Advanced THermomechanical multiscale mOdelling of Refractory linings (ATHOR) Network. These experiments were performed at 1500 °C in a biaxial press available at the Technology Centre Leoben (TCL) of RHI-Magnesita, in Austria (Fig. 7a). In this experiment, the brick units (150 × 100 × 140 mm^3) of alumina-spinel material were laid on a layer of insulation bricks. Thermal load was applied with electrical heating elements arranged near the hot face (HF) of the masonry. For the duration of thermal loads, masonry unit was free to expand. Once the desirable temperature was achieved near the HF, the loading was applied. During the load application, two sides of the rigid blocks were fixed. Relative displacement between two points (in each direction) were gathered during the experiments (Fig. 7b). Additional information regarding this extensive experimental campaign can be seen in Ref. [13]. Two different testing configurations were selected for numerical validation: a) biaxial creep test (series S06

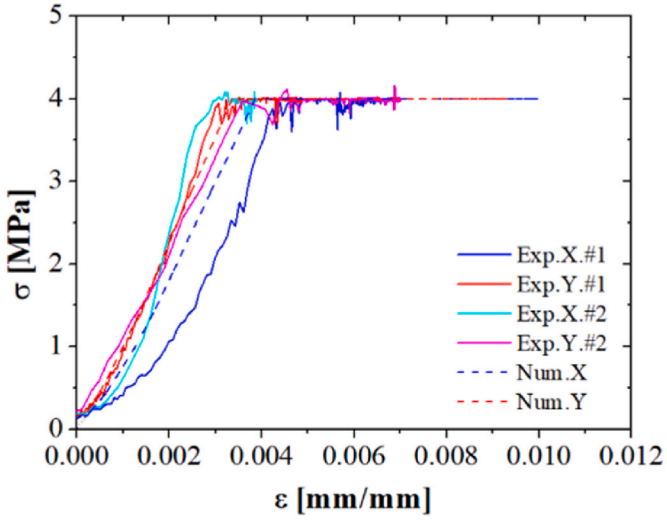

Fig. 8. Numerical vs. experimental results for the biaxial creep test.

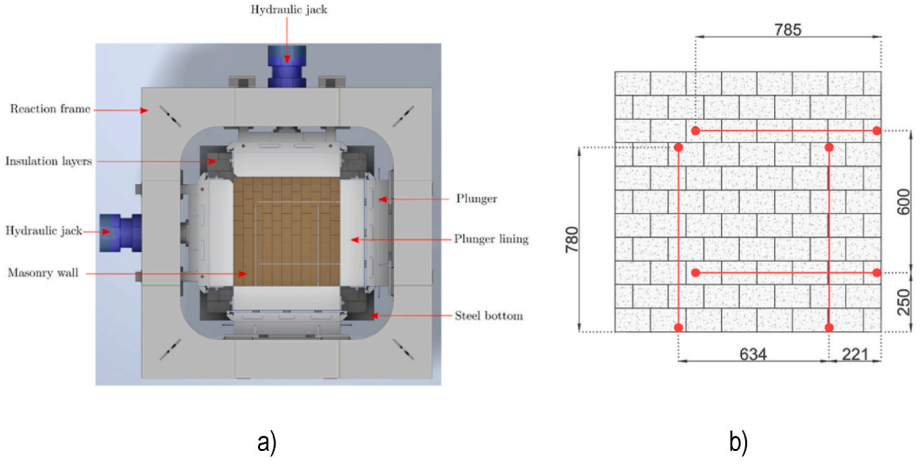

Fig. 7. Experimental setup [13]: a) schematic representation of the biaxial press; b) schematic representation of the tested specimen for biaxial creep and relaxation tests, including the arrangements of the LVDTs.

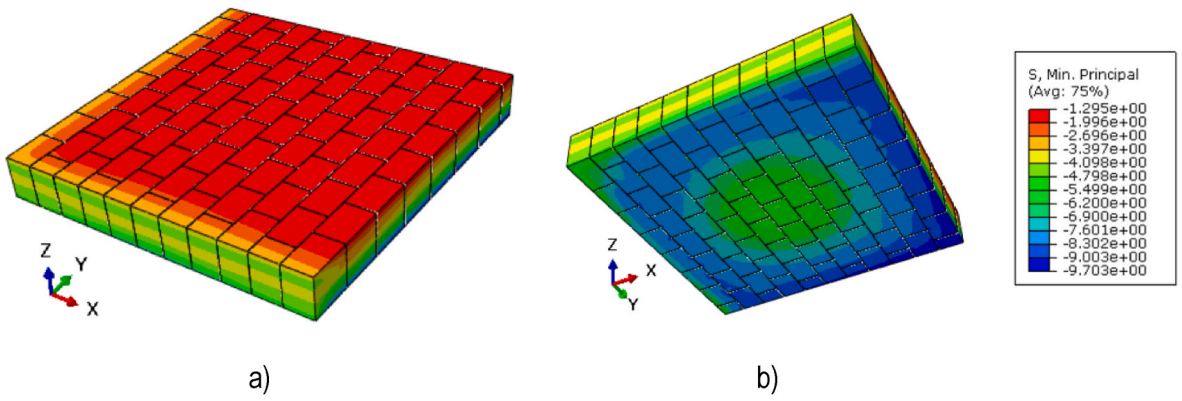

Fig. 9. Minimum principal stresses for the biaxial creep simulation [MPa]: a) hot face; b) cold face (end of the test).

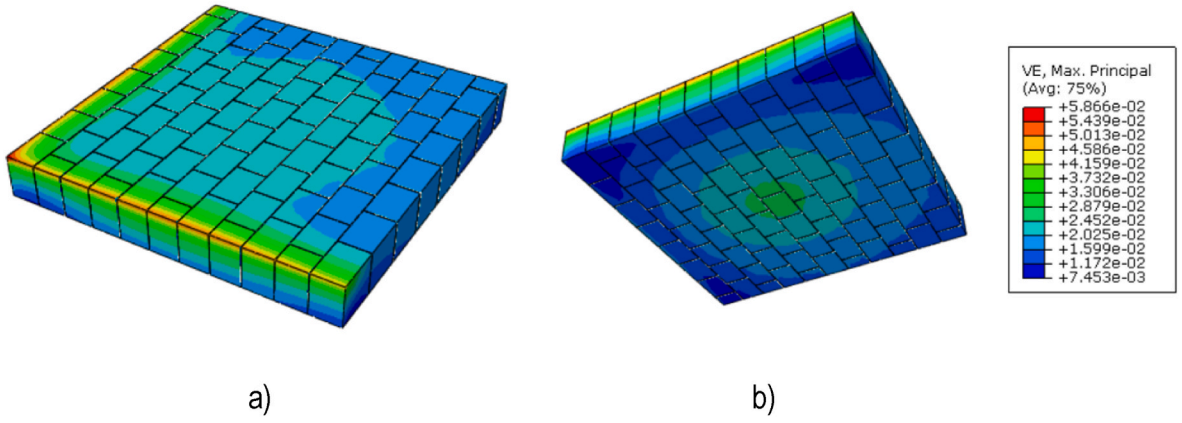

Fig. 10. Viscoplastic strains for the biaxial creep simulation: a) hot face; b) cold face (end of the test).

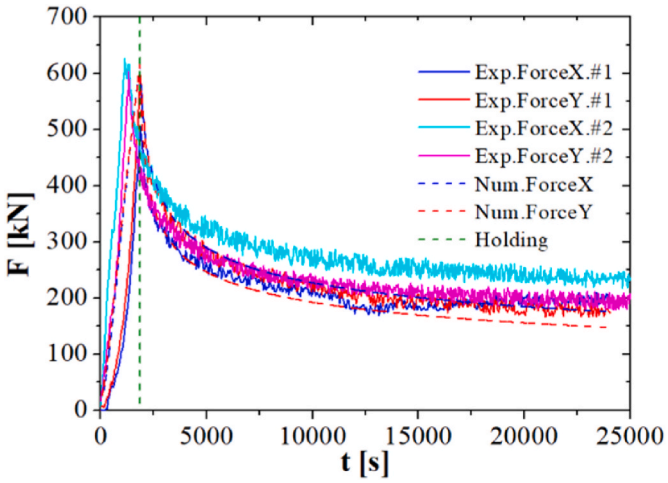

Fig. 11. Numerical vs. experimental results for the biaxial creep test.

in Ref. [13]); b) biaxial relaxation test (test S07-01 in Ref. [13]).

3.3.1. *Biaxial creep test*

The numerical and experimental results are in good agreement during the loading stage and part of the hold stage (Fig. 8). However, by the end of the test, the numerical predictions are indicating significantly higher strains. This disagreement may have been caused by the lack of characterization of the creep parameters for the temperatures below 1300 °C. The plot of the minimum principal stresses in the specimen is given in Fig. 9, at the end of the test. The largest portion of the mechanical load is being supported by the cold face of the specimen. The viscoplastic strains developed in the specimen are more significant in the hot face, and consequently, this part of the structure experiences a higher stiffness reduction (Fig. 10).

3.3.2. *Biaxial relaxation test*

The comparison of the experimental and numerical results in terms of forces versus time is given in Fig. 11. The numerical model is able to represent the reduction of the forces caused by relaxation with a good agreement. The relaxation is defined by the reduction of the mechanical stresses in the lining caused by the increase of the viscoplastic strains. The total strain is composed by the elastic, thermal and viscoplastic strain components. The mechanical load was applied to the specimens when temperature fields were stabilized (steady-state), therefore, there was no significant variation of the thermal strains. The viscoplastic strains increase during the test due to creep, and consequently, the elastic strains decreased in the same proportion. Fig. 12 presents the plot of stresses (direction X) and viscoplastic strains by the end of the load stage and by the end of the test.

As it can be seen from these two previous examples, this modelling strategy is able to properly reproduce such elements under high temperatures and complex stress states. The agreement between the numerical and experimental results is good [28].

4. Results

The numerical simulations aimed to evaluate the influence of the modelling strategy in the thermomechanical behaviour of the linings, the following comparisons have been done: a) Material modelling

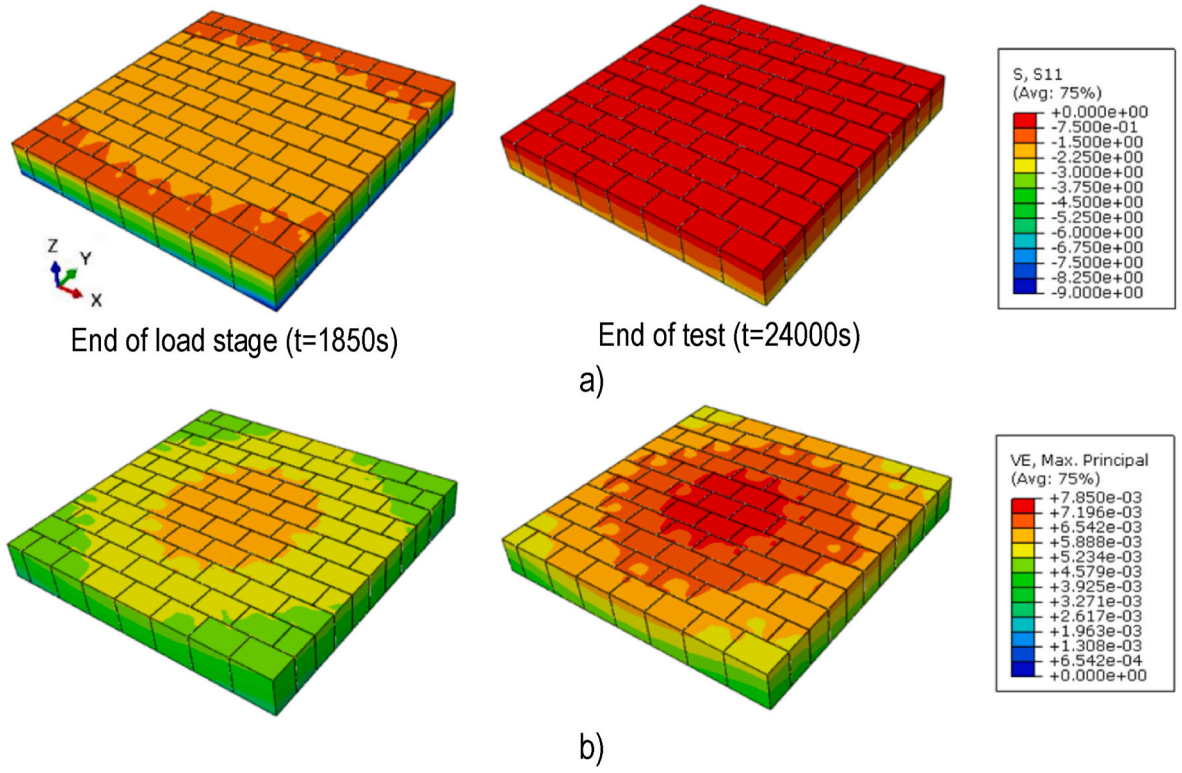

Fig. 12. Biaxial relaxation simulation: a) stress in the X direction [MPa]; b) viscoplastic strains.

Table 4
Performed simulations.

Model	Material behaviour	Joints	Young's modulus
MAE.NJ. EUS	Elastic	Isotropic (no joints)	Ultrasonic measurements
MAE.WJ. EUS	Elastic	Pressure-overclosure	Ultrasonic measurements
MAV.WJ. EUS	Viscoplastic	Pressure-overclosure	Ultrasonic measurements
MAV.WJ. ECT	Viscoplastic	Pressure-overclosure	Compressive tests

approach: elastic and viscoplastic; b) Joints modelling: perfect joint (no joint) and pressure-overclosure; c) Young's modulus characterization: obtained by ultrasonic measurements and by compressive tests. Table 4 summarizes the performed simulations. The results of the analyses are presented and analysed in this section. The temperature fields are shown and analysed in detail. Lastly, the mechanical stresses developed in the refractory linings are presented and discussed.

4.1. Temperature fields

The temperature distribution obtained in the ladle is given in Fig. 13. The maximum temperatures obtained in the working lining were 1603 °C at 16.3 h and 889 °C at 19.24 h, for the hot (P01) and cold (P02) face, respectively. The points P03 and P04 were submitted to temperatures up to 798 °C at 19.5 h and 351 °C at 20.1 h, respectively. The temperatures in the steel shell reached 260 °C by the end of the first cycle. The temperature gradient between P05 and P06 is negligible, due to the high thermal conductivity of the steel shell. Fig. 14 presents the temperatures in the ladle immediately before the pouring and tapping.

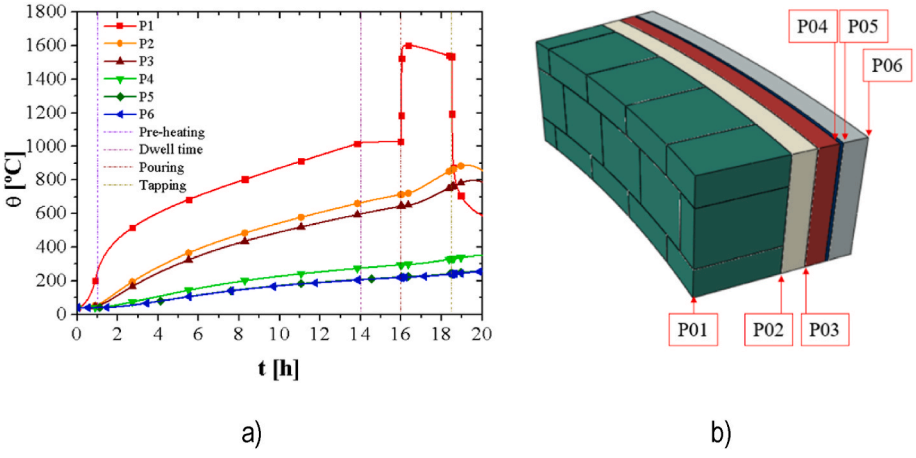

Fig. 13. Thermal response of the ladle: a) temperatures, b) location of the points.

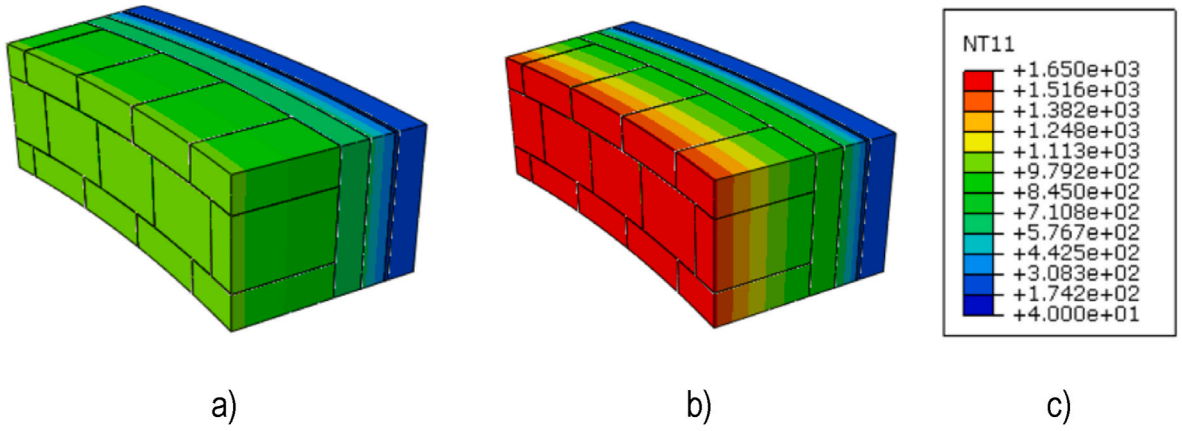

Fig. 14. Temperatures in the ladle: a) immediately before pouring, b) immediately before tapping; c) legend [in °C].

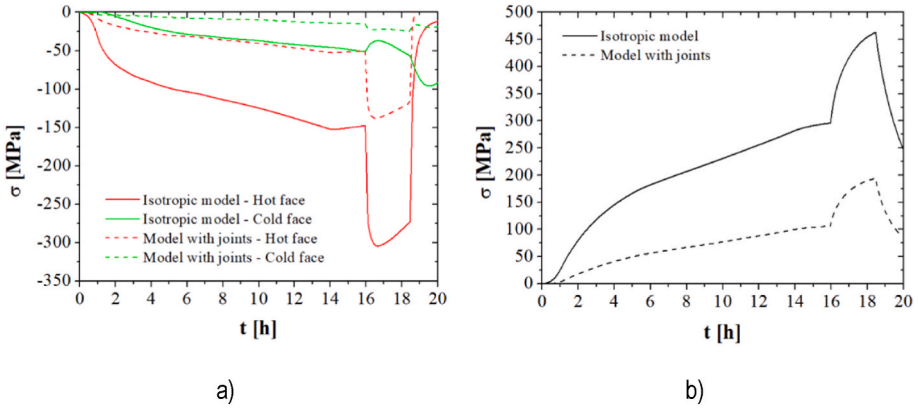

Fig. 15. Influence of the joints in the circumferential stresses developed in the ladle in a fully elastic model: a) refractory lining; b) steel shell.

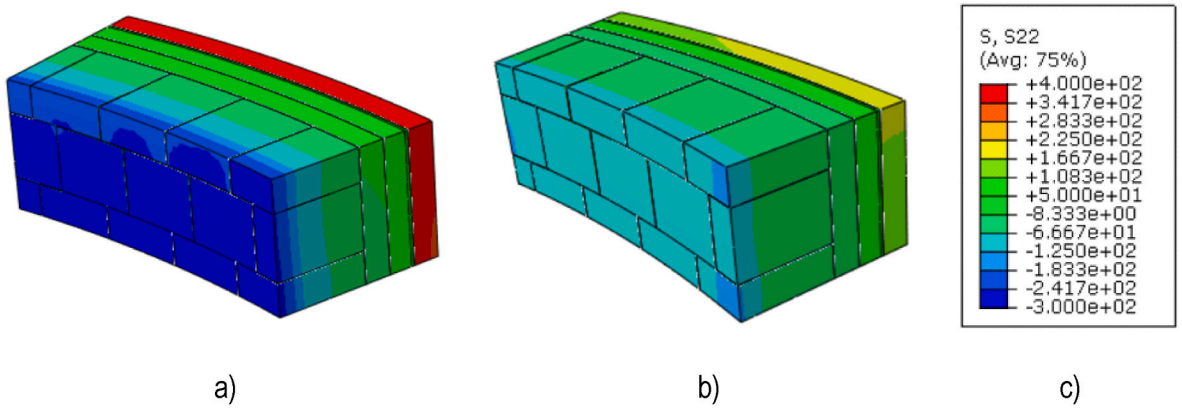

Fig. 16. Circumferential stresses in the ladle: a) isotropic model; b) model with joins; c) legend [MPa].

4.2. Stress fields

The joints played an important role in dry-stacked refractory masonries reducing the stiffness of the linings and consequently reducing the compressive stresses developed in the working layer and tensile stresses in the steel shell. The influence of the joints in a fully elastic model is being studied in this section. Fig. 15 presents the stresses predicted by the numerical models of an isotropic ladle and a ladle with joints. A significant reduction of the stresses was observed in the model with the presence of the joints. When the joints are included in the analysis, the maximum compressive stress in the hot face of the working lining decreases from 304 MPa to 132 MPa, in the cold face the compressive stress decreases from 96 MPa to 24 MPa. The tensile stresses in the steel shell decreases from 463 MPa to 194 MPa. The stresses are plot in Fig. 16 for both models.

Despite the significant reduction, the stresses developed in the refractory lining are several times higher than the material's compressive strength. Additionally, the stresses developed in the steel shell would lead to the yielding of the material. To have a better idea of the behaviour of the steel ladle, it is necessary to include the viscoplastic effects caused by creep.

The influence of the creep strains in the stresses developed in the

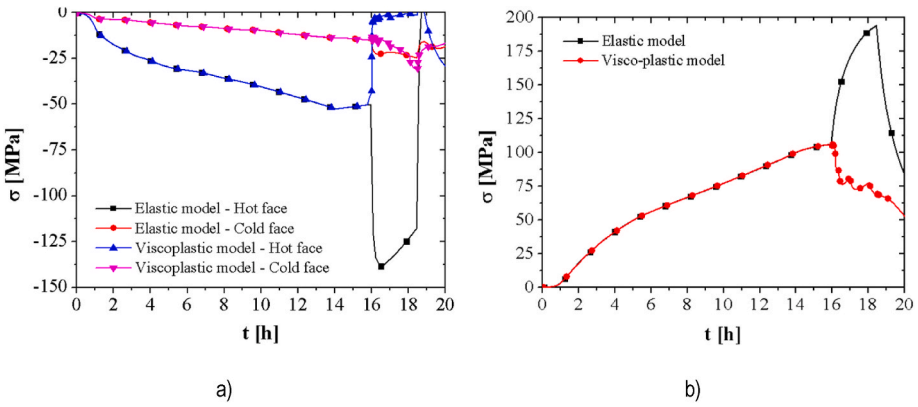

Fig. 17. Influence of the creep in the circumferential stresses developed in the ladle with joints: a) refractory lining; b) steel shell.

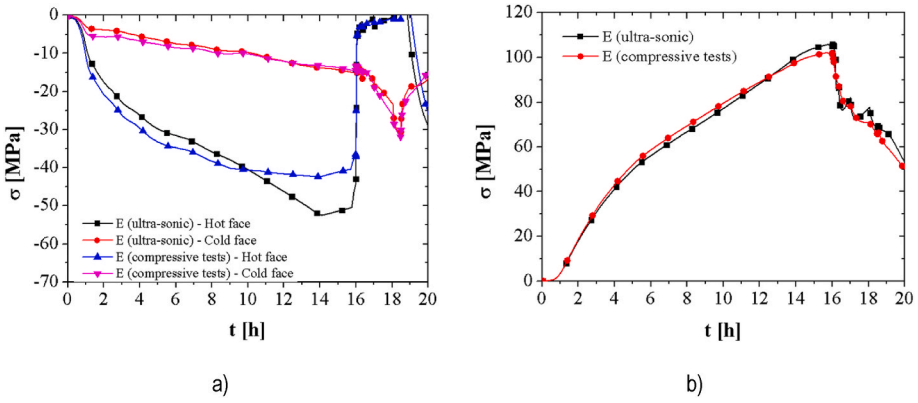

Fig. 18. Influence of the Young's modulus in the circumferential stresses developed in the ladle: a) refractory lining; b) steel shell.

steel ladle are presented in Fig. 17. The accounting of creep in the model results in a considerable stresses relief in the vessel. Due to the relaxation, the maximum compressive stress in the hot face of the working lining decreased from 132 MPa in the elastic model to 52 MPa in the viscoplastic model.

The creep strains in the hot face resulted in a slightly increase of the stresses in the cold face. This phenomenon was also observed in the numerical simulation of the ladle. The viscoplastic strains resulted in an increasing of the compressive stresses in the cold face from 24 MPa to 31 MPa. The tensile stresses in the steel shell decreased from 194 MPa to 106 MPa.

The Young's modulus of the refractory materials could be obtained by compressive tests or ultrasonic measurements. As stated by Ref. [29], above 1200 °C it was possible to observe the weakening of the material in compressive tests, this weakening was not seen in the dynamic measurements of the Young's modulus. The material was influenced by micro plastic events, which were responsible for the greater part of the deviations observed between both. Fig. 18 shows the comparison of the stresses developed in the ladle for models accounting the Young's modulus obtained by ultra-sonic technique and by compressive tests. It was possible to identify a slight reduction of the stresses in hot face from 52 MPa (ultra-sonic) to 42 MPa (compressive tests). The reduction of the stresses in the cold face and in the steel shell were not significant.

5. Conclusions

Based on the numerical simulations presented in this paper, the following conclusions may be drawn.

- The account of the joint behaviour is important for leading to reliable results of the stresses in the steel ladle. The model is sensible to the joint thickness curve used, therefore, it should be correctly determined based on compression tests in masonry wallets, as compressive tests in two stacked bricks may result in the underestimation of the joint closure curve.
- The viscoplastic strains developed in the working lining results in significant relief of the stresses (relaxation). Therefore, the creep properties of the material should be characterized under different temperatures, from 1000 °C to 1500 °C.
- The measurement of the Young's modulus by the ultrasonic technique resulted in values slightly higher than the ones obtained at the compressive tests, mostly for high temperatures. The ultrasonic technique does not account the effects of the micro plastic events that happen in the material's microstructure. Thus, the use of ultra-sonic measurements may result in the overestimation of the stresses in the ladle.
- The formulation recommended by Ref. [25] represents the evolution of the compressive stresses in the wall in terms of joint closure. The formulation was proven to be suitable for modelling the normal behaviour of dry joints presenting good results for the loading stage of the tests. However, this formulation may not be used to represent the residual strains on the unloading stage and, consequently, different pressure-overclosure relations must be used to represent the loading and unloading of masonry.
- The use of the Norton-Bailey creep law led to good results in the numerical models. The models were validated against experimental results and a good agreement was observed between them. This creep law was able to represent the behaviour of refractory lining under uniaxial creep, biaxial creep and biaxial relaxation. Nevertheless, the development of asymmetric creep models is recommended [30,31].

Declaration of competing interest

The authors declare that they have no known competing financial interests or personal relationships that could have appeared to influence the work reported in this paper

Data availability

No data was used for the research described in the article.

Acknowledgements

This work was supported by the funding scheme of the European Commission, Marie Skłodowska-Curie Actions Innovative Training Networks in the frame of the project ATHOR - Advanced THermo-mechanical multi-scale mOdelling Refractory linings 764987 Grant. The third author also acknowledges the financial support by FCT/MCTES through national funds (PIDDAC) under the R&D Unit Institute for Sustainability and Innovation in Structural Engineering (ISISE), under reference UIDB/04029/2020.

References

[1] J. Poirier, M. Rigaud, Corrosion of Refractories: the Fundamentals", F.I.R.E Compendium Series, 2017, p. 450.
[2] I. Khlifi, Optimisation of Optical Methods for Strain Field Measurements Dedicated to the Characterisation of the Fracture Behaviour of Refractories: Application to Magnesia Based Materials, in: Material Chemistry, PhD Thesis, University of Limoges, 2019, p. 182.
[3] D. Gruber, H. Harmuth, Thermomechanical behavior of steel ladle linings and the influence of insulations, Steel Res. Int. 85 (4) (2014) 512–518.
[4] K. Andreev, S. Sinnema, A. Rekik, S. Allaoui, E. Blond, A. Gasser, Compressive behaviour of dry joints in refractory ceramic masonry, Construct. Build. Mater. 34 (Sep. 2012) 402–408.
[5] S. Allaoui, A. Rekik, A. Gasser, E. Blond, K. Andreev, Digital Image Correlation measurements of mortarless joint closure in refractory masonries, Construct. Build. Mater. 162 (Feb. 2018) 334–344.
[6] R. Oliveira, J.P. Rodrigues, M. Pereira, P. Lourenco, H. Marschall, Normal and tangential behaviour of dry joints in refractory masonry, Eng. Struct. 243 (2021), 112600.
[7] A. Gasser, K. Terny-Rebeyrotte, P. Boisse, Modelling of joint effects on refractory lining behaviour," Proceedings of the Institution of Mechanical Engineers, Part L, J. Mater.: Design and Applications 218 (1) (2004) 19–28.
[8] T.M.H.H. Nguyen, E. Blond, A. Gasser, T. Prietl, Mechanical homogenisation of masonry wall without mortar, Eur. J. Mech. Solid. 28 (3) (2009) 535–544.
[9] M. Ali, T. Sayet, A. Gasser, E. Blond, Transient thermo-mechanical analysis of steel ladle refractory linings using mechanical homogenization approach, Ceramics 2 (2020) 171–188.
[10] M. Ali, T. Sayet, A. Gasser, E. Blond, Computational homogenization of elastic-viscoplastic refractor masonry with dry joints, Int. J. Mech. Sci. 196 (2021), 106275.
[11] R. Oliveira, J.P. Rodrigues, M. Pereira, P. Lourenco, H. Marschall, Thermomechanical behaviour of refractory dry-stacked masonry walls under uniaxial compression, Eng. Struct. 240 (2021), 112361.
[12] T. Prietl, Determination of Material-specific Parameters of Refractory Materials and Linings under Uniaxial and Biaxial Load Conditions for the Non-ferrous Metal Industry" - in German, Montanuniversität Leoben, Austria, 2006.
[13] M. Ali, R. Oliveira, J.M. Pereira, J.P. Rodrigues, P.B. Lourenco, M. Ulrich, T. Sayet, A. Gasser, E. Blond, Experimental characterization of the nonlinear thermomechanical behaviour of refractory masonry with dry joints, Construct. Build. Mater. 364 (2023), 129960.
[14] Z. Xia, Y. Zhang, F. Ellyin, A unified periodical boundary conditions for representative volume elements of composites and applications, Int. J. Solid Struct. 40 (2003) 1907–1921.
[15] B. Glaser, M. Gornerup, D. Sichen, Fluid flow and heat transfer in the ladle during teeming, Steel Res. Int. 82 (2011) 827–835.
[16] S. Yilmaz, Thermomechanical modelling for refractory lining of a steel ladle lifted by crane, Steel Res. Int. 74 (2003) 485–490.
[17] A. Gasser, F. Genty, J.L. Daniel, L. Chen, Influence of different masonry designs of bottom linings, in: 13th Unified International Technical Conference on Refractories, UNITECR), 2013, pp. 775–780.
[18] D. Vitiello, Material Chemistry, in: Thermo-physical Properties of Insulating Refractory Materials, PhD Thesis, University of Limoges, 2021, p. 136.
[19] D. Vitiello, D. Smith, B. Nait-Ali, N. Doyen-Tessier, T. Tonessen, L. Laim, L. Rebouillat, Thermal Properties Characterization of Refractory Materials Used in the Insulation Layer of Steel Ladles", Unified Int Tech Conf Refractories, Yokohama, Japan, 2019, pp. 205–208.
[20] R. Kaczmarek, J.C. Dupre, P. Doumalin, I.O. Pop, L.B. Teixeira, J. Gillibert, et al., Thermomechanical behaviour of an alumina spinel refractory for steel ladle applications, in: Unified International Technical Conference of Refractories, 2019, pp. 422–425. Yokohama - Japan.
[21] European Committee for Standardisation. EN 1996-1.1, Eurocode 6 – Design of Masonry Structures, Part 1.1: General Rules for Reinforced and Unreinforced Masonry Structures, 2005 (Brussels, Belgium).
[22] M. Smith, ABAQUS/Standard User's Manual, Version 2019, Dassault Systèmes Simulia Corp, United States, 2019.
[23] S. Samadi, S. Jin, H. Harmuth, Combined damaged elasticity and creep modeling of ceramics with wedge splitting tests, Ceram. Int. 47 (18) (Sep. 2021) 25846–25853.
[24] T. Zahra, M. Dhanasekar, Characterisation and strategies for mitigation of the contact surface unevenness in dry-stack masonry, Construct. Build. Mater. 169 (2018) 612–628.
[25] W. Thanoon, A. Alwathaf, J. Noorzaei, M. Jaafar, M. Abdulkadir, Finite element analysis of interlocking mortarless hollow block masonry prism, Comput. Struct. 86 (2008) 520–528.
[26] European Committee for Standardisation. EN 1996-1.2, Eurocode 6 – Design of Masonry Structures, Part 1.2, General rules Structural Fire Design", Brussels, Belgium, 2005.
[27] European Committee for Standardisation, Eurocode 3 – EN 1993-1-2 (2005) (English): Eurocode 3: Design of Steel Structures - Part 1-2, General rules - Structural fire design", Brussels, Belgium, 2005. EN 1993-1.2.
[28] R. Oliveira, Experimental and Numerical Thermomechanical Characterization of Refractory Masonries". PhD in Fire Safety Engineering, PhD Thesis, University of Coimbra, 2022, p. 260.
[29] K. Andreev, E. Zinngreve, Compressive Behaviour of ACS torpedo Bricks". 11th Unified International Technical Conference on Refractories, UNITECR, 2009.
[30] L. Teixeira, J. Gillibert, E. Blond, T. Sayet, Creep characterization of refractory materials at high temperatures using the Integrated Digital Image Correlation, in: Unified International Technical Conference of Refractories, 2019, pp. 899–902. Yokohama, Japan.
[31] L. Teixeira, S. Samadi, J. Gillibert, S. Jin, T. Sayet, D. Gruber, et al., Experimental investigation of the tension and compression creep behavior of alumina-spinel refractories at high temperatures, Ceramics 3 (3) (2020) 372–383, 2020.